IOP Publishing Journal of Physics B: Atomic, Molecular and Optical Physics
J. Phys. B: At. Mol. Opt. Phys. **47** (2014) 035203 (8pp) doi:10.1088/0953-4075/47/3/035203

Ionization of water molecules by ion beams. On the relevance of dynamic screening and the influence of the description of the initial state

C A Tachino[1], J M Monti[1], O A Fojón[1], C Champion[2] and R D Rivarola[1]

[1] Laboratorio de Colisiones Atómicas, Facultad de Ciencias Exactas, Ingeniería y Agrimensura and Instituto de Física Rosario, CONICET-Universidad Nacional de Rosario, Av Pellegrini 250, 2000 Rosario, Argentina
[2] Centre d'Etudes Nucléaires de Bordeaux Gradignan, Université Bordeaux 1, CNRS/IN2P3, CENBG, F-33175 Gradignan, France

E-mail: tachino@ifir-conicet.gov.ar

Received 21 August 2013, revised 9 December 2013
Accepted for publication 10 December 2013
Published 16 January 2014

Abstract
Single ionization from water molecules by impact of protons, alpha particles and C^{6+} ions is studied. The post- and prior-versions of the continuum distorted wave-eikonal initial state (CDW-EIS) model within an independent electron approximation are employed to compute double differential cross sections. To avoid the complexity of using numerical molecular continuum states in the cross-section calculations, effective Coulombic continuum wavefunctions are employed. However, this may lead to the appearance of post–prior discrepancies and this fact is examined in detail. Moreover, the influence of the dynamic screening on this behaviour is studied. In addition, the contribution of different molecular orbitals to the angular spectrum is analysed for several ejection electron energies. Finally, the sensitivity of CDW-EIS calculations to the representation of the initial bound molecular orbitals is investigated.

Keywords: water, ionization, ion impact, dynamic screening, post–prior discrepancies

(Some figures may appear in colour only in the online journal)

1. Introduction

Electron ionization of atoms and molecules by charged particle impact is of fundamental relevance in many areas like astrophysics and plasma physics. This process is also essential in radiobiological studies and medical physics as it is the main mechanism leading to energy loss for swift ions in the living matter at high impact energies. In order to calculate with accuracy the energy deposition by ionizing radiation in an absorbing medium, which is commonly modelled by water, a detailed description of the charged particle tracks is then needed. The determination of these patterns depends on an extensive set of total and differential cross-sections for the primary interactions of the relevant particles with the constituents of the biological tissue [1]. Then, it is important to obtain accurate theoretical and experimental cross sections for describing, in the best way, the ionization process induced by light and heavy ions on water molecules.

Besides, there is a relatively scarce number of experimental measurements devoted to the analysis of the electron ionization of isolated water molecules by the impact of bare ions. In general, published results concerning this process deal with the impact of light ions (essentially protons and alpha particles) [2–11] and to a lesser extent with the heavy ion impact [12–14].

On the theoretical side, several semi-empirical methods were employed to calculate differential and total cross sections for the ionization of vapour water [15–19]. Also, different

treatments based on the Born approximation [13, 20–25] and on the continuum distorted wave-eikonal initial state (CDW-EIS) approach [19, 26] were used to analyse the ionization reaction of water molecules, among other molecular gases, by light and heavy ion impact. Finally, let us note that concerning the first Born approximation, a review of the existing predictions for ionization and charge transfer reactions in the high-impact energy regime, for bare ions impinging on vapour and liquid water, is reported in [27].

In this paper, attention is focused on the existence of the discrepancies obtained when prior- and post-versions of the scattering amplitude are used to compute double differential cross sections (DDCS) corresponding to the ionization reaction of water molecules due to the incidence of bare ions. It is shown that these discrepancies come from the dynamic screening produced by the electrons remaining bound to the residual target on the evolution of the ionized one. Also, the role played by the representation of the initial wavefunction in the computation of DDCS is analysed. To this end, two different descriptions of the bound states of the molecular target are considered, within the post- and prior-version of the CDW-EIS model: the complete neglect of the differential overlap (CNDO) approximation, and the linear combination of atomic orbitals-self consistent field (LCAO-SCF) one provided by Moccia [28–30]. The continuum wavefunctions are represented by a double product of projectile and target Coulomb continuum factors and a plane wave. Let us add that Champion and co-workers [31] have analysed very recently the influence of the target description on the cross-section calculations for ionization and capture processes induced by heavy charged particle impact on biological targets, this study being performed within the framework of the first-order Born approximation with correct boundary conditions (CB1) and within the CDW-EIS model, together with the CNDO approach.

Atomic units will be used throughout unless otherwise stated.

2. Theory

Let us consider an incident bare ion of charge Z_P impinging on a molecular target with a velocity $\vec{v}$ parallel to the z-axis of the laboratory reference frame. The impact energies considered here are high enough, so the vibrational and rotational times of the target are much larger than the characteristic times of the collision. It is then possible to assume that the molecular nuclei remain fixed in their initial positions during the reaction. With regard to the multielectronic problem, it is reduced to the analysis of a one-active electron system by considering that all the other electrons (the passive ones) are frozen in their initial orbitals during the collision and that the active electron evolves independently of them in an effective mean field of the residual target [32].

For an electron emitted from a molecular target, DDCS as a function of the electron energy ε_k and the corresponding subtended solid angle $\Omega_k = (\theta_k, \phi_k)$ may be defined as follows:

$$\sigma^{(2)}(\varepsilon_k, \theta_k) = \frac{\mathrm{d}\sigma}{\mathrm{d}\varepsilon_k \, \mathrm{d}\Omega_k} = \frac{k}{8\pi^2} \int\int \mathrm{d}\Omega \, \mathrm{d}\vec{\rho} \, |a^{\pm}_{i,f}(\vec{\rho}, \Omega)|^2, \quad (1)$$

where the sign + (−) refers to the post- and prior-version of the transition amplitude $a_{i,f}(\vec{\rho}, \Omega)$, $\vec{k}$ is the momentum of the electron, $\vec{\rho}$ is the impact parameter vector, and Ω indicates the molecular orientation. The factor $8\pi^2$ is introduced since DDCS are averaged over all possible molecular orientations. Introducing the two-dimensional Fourier transform of $a^{\pm}_{i,f}(\vec{\rho}, \Omega)$,

$$\mathcal{R}^{\pm}_{i,f}(\vec{\eta}, \Omega) = \frac{1}{2\pi} \int \mathrm{d}\vec{\rho} \, \exp(i\,\vec{\eta} \cdot \vec{\rho}) \, a^{\pm}_{i,f}(\vec{\rho}, \Omega), \quad (2)$$

that depends on the transverse momentum transfer $\vec{\eta}$, and employing Parseval's theorem [33], DDCS can also be calculated as

$$\sigma^{(2)}(\varepsilon_k, \theta_k) = \frac{k}{8\pi^2} \int\int \mathrm{d}\Omega \, \mathrm{d}\vec{\eta} \, |\mathcal{R}^{\pm}_{i,f}(\vec{\eta}, \Omega)|^2. \quad (3)$$

Following the procedure given in [34] (see also [17, 32]), the passive electrons are supposed to affect the projectile trajectory whereas the ejected one is assumed to move independently of them. Thus, into the straight line version of the impact parameter approximation and within the distorted wave model, the first-order approximation of the transition amplitude for the active electron may be written in the post-version as

$$a^{+}_{i,f}(\vec{\rho}, \Omega) = \int_{-\infty}^{+\infty} \mathrm{d}t \, \langle \chi^{-}_f | \left(H - \mathrm{i} \frac{\partial}{\partial t} \right)\Big|^{\dagger}_{\vec{r}} \, | \chi^{+}_i \rangle \quad (4)$$

and for the prior-one as

$$a^{-}_{i,f}(\vec{\rho}, \Omega) = \int_{-\infty}^{+\infty} \mathrm{d}t \, \langle \chi^{-}_f | \left(H - \mathrm{i} \frac{\partial}{\partial t} \right)\Big|_{\vec{r}} \, | \chi^{+}_i \rangle. \quad (5)$$

In equations (4) and (5), χ^{+}_i (χ^{-}_f) represents a distorted wavefunction that satisfies correct outgoing (incoming) asymptotic boundary conditions, and H is the active-electron Hamiltonian

$$H = -\frac{\nabla^2_r}{2} + \sum_j \frac{(-Z_{T_j})}{x_j} + V_{ap}(\vec{r}) - \frac{Z_P}{s}, \quad (6)$$

where the sum runs over all the molecular nuclei with nuclear charges Z_{T_j}. Moreover, in the preceding expression, $\vec{x}_j$ is the coordinate of the jth target nucleus with respect to the laboratory reference frame, and $\vec{s}$ is the electron position vector with respect to the projectile nucleus. The term $V_{ap}(\vec{r})$ appearing in equation (6) represents the interaction between the active electron and the passive ones, this potential being averaged over the passive electron initial distributions

$$V_{ap}(\vec{r}) = \langle \varphi_p(\{\vec{r}_p\}) | \sum_p \frac{1}{|\vec{r} - \vec{r}_p|} | \varphi_p(\{\vec{r}_p\}) \rangle \quad (7)$$

with $\vec{r}$ the active electron position vector with respect to the laboratory reference frame. Also in equation (7), $\{\vec{r}_p\}$ indicates the ensemble of the passive electron positions $\vec{r}_p$, and $\varphi_p(\{\vec{r}_p\})$ represents the passive electrons wavefunction.

In the continuum distorted wave-eikonal initial state (CDW-EIS) approximation, χ^{+}_i and χ^{-}_f are chosen as

$$\chi^{+,\mathrm{EIS}}_i(\vec{r}, t) = \varphi_i(\vec{r}) \exp(-\mathrm{i}\varepsilon_i t) \, \mathcal{L}^{+,\mathrm{EIS}}_i(\vec{s}), \quad (8)$$

$$\chi^{-,\mathrm{CDW}}_f(\vec{r}, t) = \varphi_k(\vec{r}) \exp(-\mathrm{i}\varepsilon_k t) \, \mathcal{L}^{-,\mathrm{CDW}}_f(\vec{s}), \quad (9)$$

with φ_i (φ_k) the bound (continuum) wavefunction of the active electron, ε_i is the active-electron orbital energy and $\varepsilon_k = k^2/2$. Eikonal and continuum distortion factors, associated with the presence of the electron in the field of the projectile, introduced in equations (8) and (9), are given by the expressions

$$\mathcal{L}_i^{+,\mathrm{EIS}}(\vec{s}) = \exp[-\mathrm{i}\nu \ln(vs + \vec{v}\cdot\vec{s})], \tag{10}$$

$$\mathcal{L}_f^{-,\mathrm{CDW}}(\vec{s}) = N(\varsigma)\,{}_1F_1[-\mathrm{i}\varsigma;\,1;\,-\mathrm{i}(ps + \vec{p}\cdot\vec{s})], \tag{11}$$

respectively, where $\nu = Z_P/v$, $\varsigma = Z_P/p$ with $\vec{p} = \vec{k} - \vec{v}$ the momentum of the electron considered with respect to a reference frame centred on the projectile nucleus, and $N(a) = \exp(a\pi/2)\,\Gamma(1 + \mathrm{i}\,a)$, with ${}_1F_1(b;\,c;\,z)$ the Kummer confluent hypergeometric function.

In order to avoid the complexity of the use of numerical three-centre molecular continuum wavefunctions, the active electron-residual target potential in the exit channel is approximated by an effective Coulomb one

$$V_T(\vec{r}) = \sum_j \frac{(-Z_{T_j})}{x_j} + V_{ap}(\vec{r}) \approx -\frac{Z_T^*}{r}, \tag{12}$$

where Z_T^* is an effective charge. This charge is chosen in correspondence with the energy of each one of the orbitals composing the molecule. Moreover, in expression (4), a residual perturbative potential

$$V_r(\vec{r}) = \left(\sum_j \frac{(-Z_{T_j})}{x_j} + \frac{Z_T^*}{r}\right) + V_{ap}(\vec{r}) \tag{13}$$

is usually neglected for ionization of atomic targets. This term contains the influence of the passive electron on the dynamical evolution of the active one that is only partially taken into account in the potential $-Z_T^*/r$. Thus, the residual target continuum state of the emitted electron is written as

$$\varphi_k(\vec{r}) = (2\pi)^{-3/2} \times \exp(\mathrm{i}\,\vec{k}\cdot\vec{r})\,N(\xi)\,{}_1F_1(-\mathrm{i}\,\xi;\,1;\,-\mathrm{i}\,k\,r - \mathrm{i}\,\vec{k}\cdot\vec{r}), \tag{14}$$

with $\xi = Z_T^*/k$. This effective Coulomb target continuum state was applied with certain success to describe single ionization in many high-energy collision systems involving ion beams and atomic targets [17, 35].

From the neglection of (13) in (4), it is therefore evident that even though the same initial and final distorted wavefunctions were considered, DDCS calculations performed with the post- and prior-versions of the model would give different results. In the literature this is known as the so-called post–prior discrepancies [36].

The initial wavefunction φ_i of the active electron bound to a particular molecular orbital MO is described employing two different descriptions. In the CNDO approximation originally developed by Pople *et al* [37–39], molecular orbitals for the valence electrons were proposed to be written as a LCAO, the basis set being employed to this end is a minimal one consisting of Slater-type functions (STF) with fixed characteristic exponent values. On the other hand, all inner shells were treated as a part of an unpolarized core. But within this description, some difficulties appear in the calculation of $\sigma^{(2)}(\varepsilon_k, \Omega_k)$, since all the crossed-terms between different atomic orbitals should be obtained. To simplify the computation of the DDCS, then we make use of the method proposed by Senger *et al* [20, 21]. In this treatment, all the overlapping integrals are neglected and the resulting DDCS for any MO is then reduced to a weighted sum of atomic DDCS corresponding to the atomic constituents of the molecule. Then, for the particular case of water, whose electronic configuration in the fundamental state is $(1a_1)^2(2a_1)^2(1b_2)^2(3a_1)^2(1b_1)^2$, double differential cross section for the complete molecule can be calculated as

$$\sigma^{(2)}_{\mathrm{H_2O}} = \sigma^{(2)}_{1a_1} + \sigma^{(2)}_{2a_1} + \sigma^{(2)}_{1b_2} + \sigma^{(2)}_{3a_1} + \sigma^{(2)}_{1b_1}, \tag{15}$$

where

$$\sigma^{(2)}_{1a_1} = 2 \times \sigma^{(2)}_{O_{1s}}, \tag{16}$$

$$\sigma^{(2)}_{2a_1} = 1.48 \times \sigma^{(2)}_{O_{2s}} + 0.52 \times \sigma^{(2)}_{H_{1s}}, \tag{17}$$

$$\sigma^{(2)}_{1b_2} = 1.18 \times \sigma^{(2)}_{O_{2p}} + 0.82 \times \sigma^{(2)}_{H_{1s}}, \tag{18}$$

$$\sigma^{(2)}_{3a_1} = 0.22 \times \sigma^{(2)}_{O_{2s}} + 1.44 \times \sigma^{(2)}_{O_{2p}} + 0.34 \times \sigma^{(2)}_{H_{1s}}, \tag{19}$$

$$\sigma^{(2)}_{1b_1} = 2 \times \sigma^{(2)}_{O_{2p}}. \tag{20}$$

The atomic orbital populations presented in equations (16)–(20), which were calculated within the CNDO approach, were taken from [40]. The corresponding orbital energies are: $\varepsilon_i^{(1a_1)} = -19.842$ au, $\varepsilon_i^{(2a_1)} = -1.18$ au, $\varepsilon_i^{(1b_2)} = -0.67$ au, $\varepsilon_i^{(3a_1)} = -0.54$ au and $\varepsilon_i^{(1b_1)} = -0.46$ au. In the calculation of the atomic DDCS that appear in equations (16)–(20), the initial bound wavefunctions were described by Slater-type orbitals [41]. The effective charge Z_T^* introduced in equation (12), is chosen as $Z_T^* = \sqrt{-2\,n\,\varepsilon_i}$, where n is the principal quantum number of each atomic compound that constitutes the considered initial molecular orbital of the active electron, and ε_i is the corresponding orbital energy.

The second approximation considered in this work was developed by Roberto Moccia [28–30]. In this approach, the ground state orbitals of molecules of the type XH_n were constructed from a linear combination of STF all referred to a common origin. This point was chosen to be located at the position of the nucleus of the atom labelled X, since in these types of molecules—which have a strong monocentric character—the electronic cloud is located mainly around it. However, these wavefunctions were derived for a particular orientation of the molecule in space, but in experimental conditions is unlikely to find oriented targets. Therefore, to compare our theoretical results with the existing experimental data, it is necessary to work with a randomly oriented molecule. Let us consider that $\vec{r}_0 = (r, \Omega_0)$ represents the electron coordinate with respect to the origin of the laboratory reference frame corresponding to the orientation analysed by Moccia. The bound state $\varphi_i(\vec{r}_0)$ can be written in the following way:

$$\varphi_i(\vec{r}_0) = \sum_{j=1}^{N} a_{n_j l_j m_j}\,\psi^{\mathrm{STO}}_{n_j l_j m_j}(\xi_{n_j l_j m_j}, \vec{r}_0), \tag{21}$$

with a_{nlm} the coefficient of the linear combination associated with the quantum numbers (n, l, m), and $\psi^{\mathrm{STO}}_{nlm}$ the STF,

$$\psi^{\mathrm{STO}}_{nlm}(\xi_{nlm}, \vec{r}_0) = R_{nl}(\xi_{nlm}, r)\,S_{lm}(\Omega_0). \tag{22}$$

In the above expression, ξ_{nlm} is the STO characteristic exponent, R_{nl} is the radial function, and S_{lm} represents a real spherical harmonic that can be expressed as a linear combination of complex spherical harmonics $Y_l^{m'}$,

$$S_{lm}(\Omega) = b_{1,m}\, Y_l^{-|m|}(\Omega) + b_{2,m}\, Y_l^{|m|}(\Omega) + b_{3,m} Y_l^0(\Omega), \quad (23)$$

with the coefficients $b_{j,m}$ $(j = 1,\ 2,\ 3)$ given by

$$b_{1,m} = \left(\frac{m}{2|m|}\right)^{1/2} (1 - \delta_{m,0}), \quad (24)$$

$$b_{2,m} = (-1)^{|m|} 2 \left(\frac{m}{2|m|}\right)^{3/2} (1 - \delta_{m,0}), \quad (25)$$

$$b_{3,m} = \delta_{m,0}. \quad (26)$$

In equations (24)–(26), the symbol $\delta_{i,j}$ represents the Kronecker delta.

An arbitrary oriented wavefunction $\varphi_i(\vec{r})$ may be obtained by applying the rotation operator $\mathfrak{D}(\alpha, \beta, \gamma)$ [42], depending on the Euler angles (α, β, γ), on expression (21).

After some algebra, it is possible to demonstrate that the post- and prior-versions of the scattering matrix element $\mathcal{R}_{i,f}^{\pm,\mathrm{CDW-EIS}}(\vec{\eta})$ may be expressed as

$$\mathcal{R}_{i,f}^{\pm,\mathrm{CDW-EIS}}(\vec{\eta}) = \sum_{j=1}^{N} \sum_{\mu_j=-l_j}^{l_j} a_{n_j l_j m_j} \left[b_{1,m_j}\, \mathcal{D}^{(l_j)}_{\mu_j,-|m_j|}(\alpha,\beta,\gamma) + b_{2,m_j} \mathcal{D}^{(l_j)}_{\mu_j,|m_j|}(\alpha,\beta,\gamma) + b_{3,m_j}\, \mathcal{D}^{(l_j)}_{\mu_j,0}(\alpha,\beta,\gamma) \right] \times \mathcal{R}^{\pm,\mathrm{CDW-EIS}}_{n_j,l_j,m_j}(\vec{\eta}), \quad (27)$$

where $\mathcal{R}^{\pm,\mathrm{CDW-EIS}}_{nlm}(\vec{\eta})$ is an effective scattering matrix element related to an atomic orbital with quantum numbers (n, l, m), and $\mathcal{D}^{(l)}_{\mu,m}(\alpha, \beta, \gamma)$ is the rotation matrix element [42]. Taking into account that the rotation matrix element $\mathcal{D}^{(l)}_{\mu,m}(\alpha, \beta, \gamma)$ satisfies the orthogonality property, it can be demonstrated that DDCS for single ionization from a molecular orbital (MO) are given by

$$\sigma^{(2)}_{\mathrm{MO}}(\varepsilon_k, \Omega_k) = \sum_{j=1}^{N} \sum_{\mu_j=-l_j}^{l_j} \sum_{j'=1}^{N} \sum_{\mu_{j'}=-l_{j'}}^{l_{j'}} \frac{k}{2\,l_j + 1}\, a_{n_j l_j m_j}\, a_{n_{j'} l_{j'} m_{j'}} \times \left[(b_{1,m_j}\, b_{1,m_{j'}} + b_{2,m_j}\, b_{2,m_{j'}}) \delta_{|m_j|,|m_{j'}|} + b_{3,m_j}\, b_{3,m_{j'}} \right] \times \int \mathrm{d}\vec{\eta}\, \mathcal{R}^{\pm,\mathrm{CDW-EIS}}_{n_j l_j m_j}(\vec{\eta})\, \mathcal{R}^{\pm,\mathrm{CDW-EIS}^*}_{n_{j'} l_{j'} m_{j'}}(\vec{\eta}). \quad (28)$$

DDCS for the complete molecule are computed by summing the contributions from all molecular orbitals,

$$\sigma^{(2)}(\varepsilon_k, \Omega_k) = \sum_{\mathrm{MO}} N_{el_{\mathrm{MO}}}\, \sigma^{(2)}_{\mathrm{MO}}(\varepsilon_k, \Omega_k), \quad (29)$$

with $N_{el_{\mathrm{MO}}}$ the corresponding orbital occupation numbers.

3. Results and discussion

Discrepancies arising from the use of the post- and prior-versions of the transition amplitude in the description of the single ionization reaction of water molecules due to the impact of bare ions are investigated. To this end, a comparison between double differential ionization cross-sections calculated by employing both formulations is presented.

Theoretical electron angular distributions calculated with the post-formulation (post-DDCS) and with the prior-one (prior-DDCS) corresponding to the collision between 4.5 MeV/u-O^{8+} ions and water molecules, as a function of the electron emission angle and for emission energies ε_k = 20, 40, 100, 200, 240 and 320 eV are presented in figure 1, together with experiments [14]. Both post- and prior-forms of CDW-EIS are compared, considering the initial bound state of the active electron described by Moccia wavefunctions. From the comparison between these results, it can be seen that prior-DDCS exhibit a better agreement with experiments than the post-ones, indicating a clear evidence of post–prior discrepancies. Recently, the same effect was observed in post- and prior-CNDO calculations for this system [14] and also in the case of 6 MeV/u-C^{6+} impact (results not shown here) [43, 44], when Roothaan–Hartree–Fock (RHF) wavefunctions [45] were used instead of Slater-type orbitals in the CNDO approximation to compute the atomic-DDCS. The differences between both sets of results can be attributed to the fact that in the prior-version the influence of the passive electrons on the dynamical evolution of the ejected one (the so-called dynamical screening) is implicitly included, whereas in the post-version it is only partially taken into account through the use of an effective charge in the final continuum representation [46, 47].

In order to give evidence of this effect, we analyse the less bound $1b_1$ orbital and the tighter one $1a_1$. Both orbitals correspond in a CNDO analysis to O_{2p} and O_{1s} atomic states (see expressions (16)–(20)). Following a recent work [48], where dynamic screening for atomic targets was investigated, we describe the residual perturbative potential given in equation (13) by a Green–Sellin–Zarcher (GSZ) parametric one. Results obtained considering the inclusion of the GSZ potential in the calculation of the post-DDCS are presented in figure 2. In this case, RHF wavefunctions [45] were used to represent the atomic states. According to figure 2, an almost total agreement between the prior-version and this 'complete' post-one of CDW-EIS is obtained. This gives evidence that post–prior discrepancies are due to the influence of passive electrons on the dynamical evolution of the ionized one.

In figure 3, the contribution of different orbitals to the DDCS is discriminated for impact of 6 MeV/u-C^{6+} on vapour water. Prior-version CDW-EIS calculations are presented for different electron ejection energies. At the lower ejection energy considered (ε_k = 19.2 eV), the preference for ionization is ordered according to the initial orbital bound energy, decreasing the contributions from the less bound electrons in the $1b_1$ orbital to the more bound ones. However, as the ejected electron energy increases, all orbitals start to compete, so that for ε_k = 384 eV, the tighter electrons (which correspond to the $1a_1$ orbital) dominate the DDCS at forward and backscattering emission angles. This behaviour can be explained by the fact that high energy electron emission should be preferable from inner orbitals, considering that in these states electrons possess higher linear momentum. We

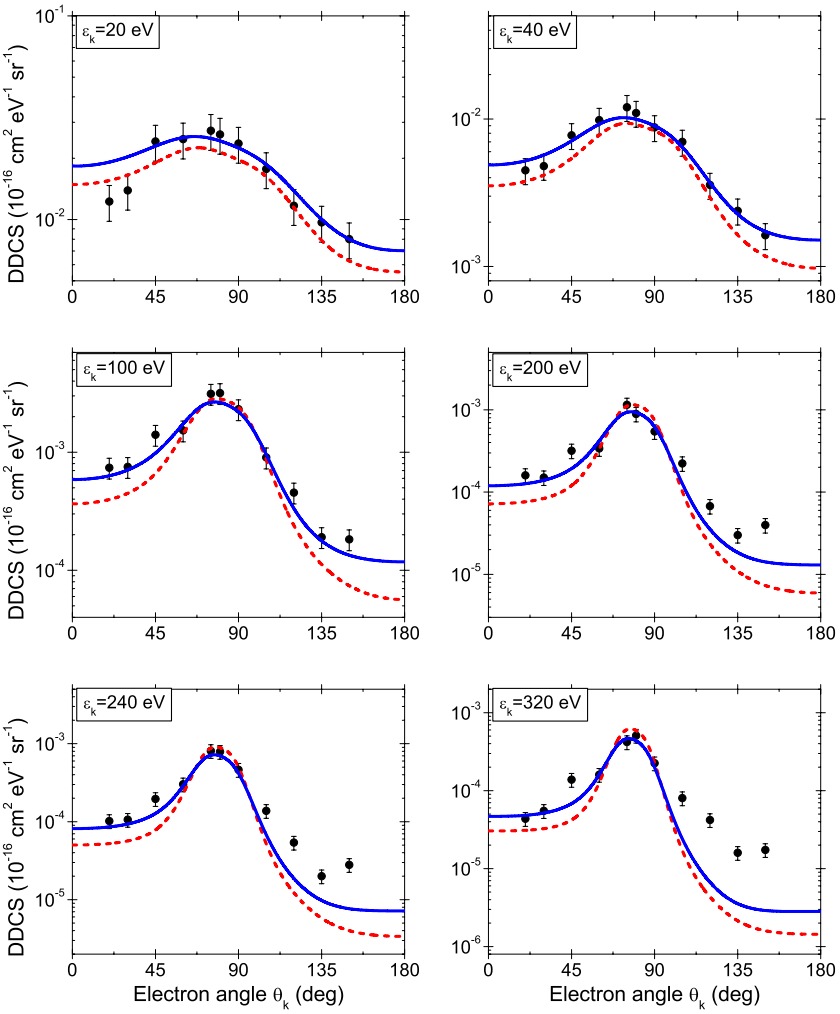

Figure 1. Angular distributions for the single ionization of H_2O by the impact of 4.5 MeV/u-O^{8+}, as a function of the emission angle and for different electron emission energies. Dashed red lines correspond to post-DDCS, whereas solid blue lines represent prior-DDCS. All the theoretical results were calculated with the Moccia representation of the bound state of the active electron. Filled circles represent experimental data taken from [14].

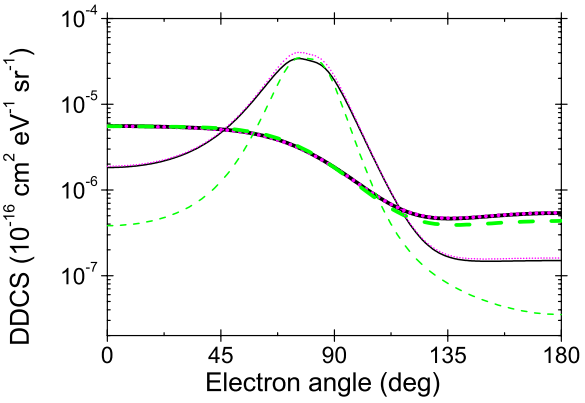

Figure 2. DDCS for the impact of 6 MeV/u-C^{6+} corresponding to the $1a_1$ and $1b_1$ molecular orbitals for electron emission energy $\varepsilon_k = 384$ eV, calculated with the post- and prior-versions within the CNDO approach. Molecular orbital $1a_1$: prior-DDCS (solid black line), post-DDCS (dashed green line), complete post-DDCS (dotted pink line). Molecular orbital $1b_1$: prior-DDCS (thin solid black line), post-DDCS (thin dashed green line), complete post-DDCS (thin dotted pink line).

should remind that for charged particles impact, the collision is produced by the momentum exchange from the projectile to the target. Moreover, at the high-impact energies considered here, the charged projectile can penetrate easily in the region of the inner orbitals of the molecule. All the other orbitals contribute in a comparable way at the binary encounter peak, dominating the DDCS in the corresponding angular region. Considering that the orbital energy of the $1a_1$ orbital is more than one order of magnitude larger than the ones corresponding to the other orbitals, the less bound ones present a more pronounced binary encounter character.

In the second part of our work, the influence of the characterization of the initial bound state of the active electron in the description of the single ionization reaction of water is investigated for some collision systems. To this end, a comparison between double differential ionization cross sections for water molecules described by employing either the Moccia representation of the electronic initial states or the ones calculated within the Senger method with CNDO populations is presented.

DDCS as a function of the emission angle θ_k, for fixed values of the emitted electron energy ε_k, for single electron

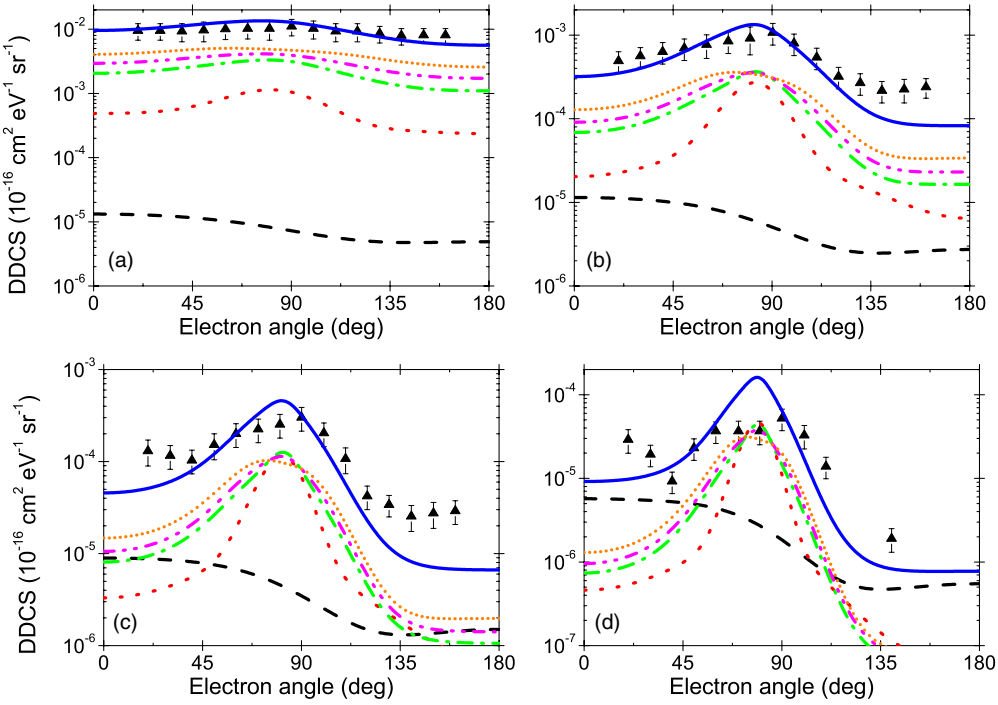

Figure 3. Prior-DDCS molecular orbital contributions for the impact of 6 MeV/u-C^{6+} on water, as a function of the electron emission angle θ_k and for fixed values of the electron emission energy ε_k: (a) $\varepsilon_k = 19.2$ eV, (b) $\varepsilon_k = 96.2$ eV, (c) $\varepsilon_k = 192$ eV, (d) $\varepsilon_k = 384$ eV. Theory: DDCS for the complete molecule (solid line); $1a_1$ contribution (dashed line); $2a_1$ contribution (dotted line); $1b_2$ contribution (dash-dotted line); $3a_1$ contribution (dash-dot-dotted line); $1b_1$ contribution (short dotted line). All the theoretical results were calculated within the CNDO approach. Experiments (triangles) taken from [13].

ionization of water were computed. Post-DDCS (calculated without the residual perturbative potential of equation (13)) for impact of protons, alpha particles and C^{6+} ions are shown in figures 4(a)–(d). Experiments are also shown for comparison [2, 13, 23].

In general, it seems that differences between both initial state descriptions are not significative over all the angular range. For proton and C^{6+} ion incidence (see figures 4(a) and (d), respectively), Moccia's results show in general a small enhancement with respect to the CNDO ones in the region of backward angles for all the considered electron emission energies. This behaviour is also observed for forward emission but only in the heaviest ion impact case and for the values of ε_k larger than 96.2 eV. On the other hand, from the curves plotted in figures 4(b) and (c) it can be seen that both sets of theoretical results are so close that they are almost indistinguishable when the collision with alpha particle projectiles is studied. Therefore, it can be concluded that CDW-EIS is not too sensitive to the description of the initial bound state of the emitted electron when the post-version of DDCS is calculated. This behaviour may be explained from the fact that in the post-version, the perturbation operator acts over the final state of the ionized electron, and the continuum wavefunctions employed in both Moccia and CNDO descriptions consider essentially almost the same functions.

In figures 5(a)–(d), prior-DDCS for the same collision systems presented in figure 4 are plotted. It can be seen that CNDO results are slightly larger than the ones corresponding to Moccia's results for electron emission energies lower than 100 eV, whereas the opposite comportment is observed for $\varepsilon_k > 100$ eV. It can be said then that as it happens for post-DDCS, the initial representation of the molecular orbitals does not have a noticeable influence in the prior-version calculation of DDCS. This behaviour can be explained by the fact that actually, the STO basis sets employed in both theoretical approximations are not too different from each other. Although Moccia's basis set is larger than the minimal one used in the CNDO method, the corresponding coefficients for STO with $n > 2$ are in general much smaller than those with $n \leqslant 2$. The molecular orbital $1b_2$ is the only exception, since the contribution of 3d-type functions is not negligible compared with the contribution of the 1s, 2s and 2p ones.

A better agreement with measurements is obtained when the prior-version of CDW-EIS is employed. This was observed previously for atomic targets [36, 46, 48]. It should also be noted that CB1 calculations (not shown here for clarity reasons) [13, 22, 23] obtained within a prior-version present in general a better accordance with experimental data than CDW-EIS results for backscattering angles. However, the reverse situation is observed when forward scattering is studied, in particular when the velocities of the projectile and the ionized electron are comparable. This can be expected from the fact that CDW-EIS is a two-centre approximation that considers on equal footing the influence of the projectile and target fields on the ejected electron. Moreover, CB1 calculations appears to be more sensitive than CDW-EIS ones to the description of the initial state [31].

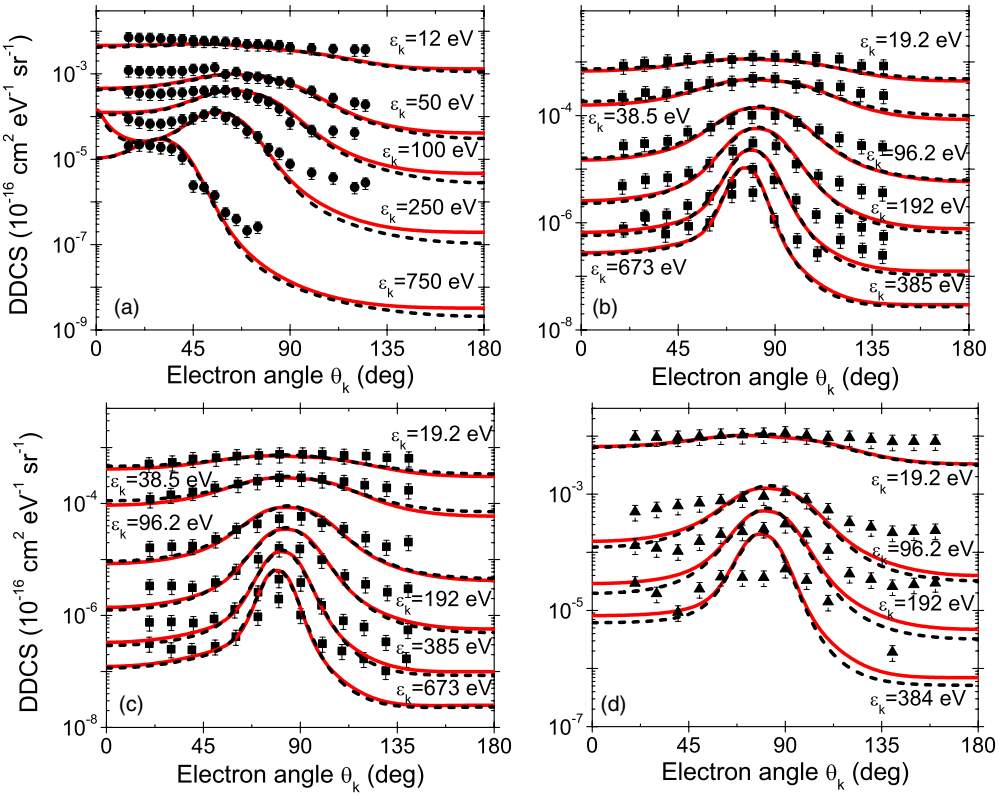

Figure 4. Post-DDCS as a function of the electron emission angle θ_k and for fixed values of the electron emission energy ε_k for single ionization of H_2O by impact of: (a) 500 keV-H^+, (b) 6 MeV/u-He^{2+}, (c) 10 MeV/u-He^{2+} and (d) 6 MeV/u-C^{6+}. Solid red lines: DDCS obtained with the Moccia description. Dashed black lines: DDCS calculated with CNDO populations. Experiments: circles [2], squares [23], triangles [13].

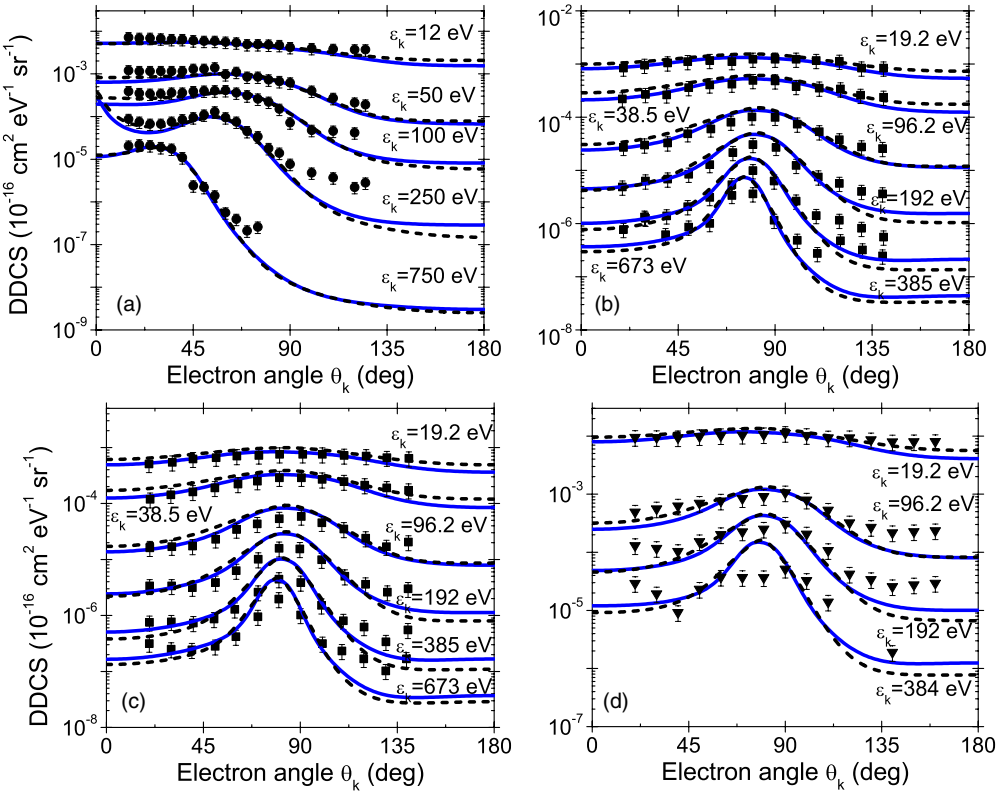

Figure 5. Same as figure 4 but for prior-DDCS (solid blue lines corresponds to Moccia's description).

4. Conclusions

Single electron ionization of water molecules by the impact of fast ion beams was investigated. The use of effective Coulombic target Coulomb continuum wavefunctions instead of numerical ones, introduced to simplify CDW-EIS DDCS calculations, gives place to post–prior discrepancies as observed for atomic targets. It is proved that these discrepancies can be almost completely diminished if the dynamic screening is properly included in the post-version. Then, the prior-version appears as a good candidate to describe the reaction.

Moreover, it is shown that electron ionization can be dominated by the different molecular orbitals depending on the final electron angular and energy conditions. In addition, DDCS are found to be not very sensitive to the molecular initial state description.

Future work is focused on a more complete representation of the final continuum state for molecules with strong monocentric character.

Acknowledgments

CAT, JMM, OAF and RDR acknowledge the CONICET (PIP 11220090101026) and the project PICT 2145 of the Agencia Nacional de Promoción Científica y Tecnológica. This work was partially supported by the ECOS-Sud A09E04, and by the project PICS 5921 (THEOS) of the Centre National de la Recherche Scientifique.

References

[1] Champion C, L'Hoir A, Politis M F, Fainstein P D, Rivarola R D and Chetioui A 2005 *Rad. Res.* **163** 222
[2] Toburen L H and Wilson W E 1977 *J. Chem. Phys.* **66** 5202
[3] Toburen L H, Wilson W E and Popowich R J 1980 *Rad. Res.* **82** 27
[4] Rudd M E, Goffe T V, DuBois R D and Toburen L H 1985 *Phys. Rev.* A **31** 492
[5] Rudd M E, Itoh A and Goffe T V 1985 *Phys. Rev.* A **32** 2499
[6] Bolorizadeh M A and Rudd M E 1986 *Phys. Rev.* A **33** 888
[7] Werner U, Beckord K, Becker J and Lutz H O 1995 *Phys. Rev. Lett.* **74** 1962
[8] Gobet F, Farizon B, Farizon M, Gaillard M J, Carré M, Lezius M, Scheier P and Märk T D 2001 *Phys. Rev. Lett.* **86** 3751
[9] Gobet F *et al* 2004 *Phys. Rev.* A **70** 062716
[10] Ohsawa D, Kawauchi H, Hirabayashi M, Okada Y, Honma T, Higashi A, Amano S, Hashimoto Y, Soga F and Sato Y 2005 *Nucl. Instrum. Methods Phys. Res.* B **227** 431
[11] Ohsawa D, Sato Y, Okada Y, Shevelko V P and Soga F 2005 *Phys. Rev.* A **72** 062710
[12] Ohsawa D, Tawara H, Okada T, Soga F, Galassi M E and Rivarola R D 2012 *J. Phys.: Conf. Ser.* **388** 102029
[13] Dal Capello C, Champion C, Boudrioua O, Lekadir H, Sato Y and Ohsawa D 2009 *Nucl. Instrum. Methods Phys. Res.* B **267** 781
[14] Nandi S, Biswas S, Khan A, Monti J M, Tachino C A, Rivarola R D, Misra D and Tribedi L C 2012 *Phys. Rev.* A **87** 052710
[15] Rudd M E 1989 *Int. J. Radiat. Appl. Instrum. Part D. Nucl. Tracks Radiat. Meas.* **16** 213
[16] Hansen J P and Kocbach L 1989 *J. Phys. B: At. Mol. Opt. Phys.* **22** L71
[17] Stolterfoht N, DuBois R D and Rivarola R D 1997 *Electron Emission in Heavy Ion–Atom Collisions* (Berlin: Springer)
[18] Bernal M A and Liendo J A 2006 *Nucl. Instrum. Methods Phys. Res.* B **251** 171
[19] Bernal M A and Liendo J A 2007 *Nucl. Instrum. Methods Phys. Res.* B **262** 1
[20] Senger B, Wittendorp-Rechenmann E and Rechenmann R V 1982 *Nucl. Instrum. Methods Phys. Res.* B **194** 437
[21] Senger B and Rechenmann R V 1984 *Nucl. Instrum. Methods Phys. Res.* B **2** 204
[22] Boudrioua O, Champion C, Dal Cappello C and Popov Y V 2007 *Phys. Rev.* A **75** 022720
[23] Champion C, Boudrioua O, Dal Cappello C, Sato Y and Ohsawa D 2007 *Phys. Rev.* A **75** 032724
[24] Champion C, Boudrioua O and Dal Cappello C 2008 *J. Phys.: Conf. Ser.* **101** 012010
[25] Champion C and Dal Cappello C 2009 *Nucl. Instrum. Methods Phys. Res.* B **267** 881
[26] Olivera G H, Fainstein P D and Rivarola R D 1996 *Phys. Med. Biol.* **41** 1633
[27] Champion C, Hanssen J and Rivarola R D 2013 *Advances in Quantum Chemistry* vol 65 (Oxford: Elsevier)
[28] Moccia R 1964 *J. Chem. Phys.* **40** 2164
[29] Moccia R 1964 *J. Chem. Phys.* **40** 2176
[30] Moccia R 1964 *J. Chem. Phys.* **40** 2186
[31] Champion C, Galassi M E, Weck P F, Fojón O A, Hanssen J and Rivarola R D 2012 *Radiation Damage in Biomolecular Systems. Biological and Medical Physics. Biomedical Engineering* (Berlin: Springer)
[32] Fainstein P D, Ponce V H and Rivarola R D 1988 *J. Phys. B: At. Mol. Opt. Phys.* **21** 287
[33] Crothers D S F and McCann J F 1983 *J. Phys. B: At. Mol. Phys.* **16** 3229
[34] Fainstein P D, Ponce V H and Rivarola R D 1991 *J. Phys. B: At. Mol. Opt. Phys.* **24** 3091
[35] Rivarola R D and Fainstein P D 2003 *Nucl. Instrum. Methods Phys. Res.* B **205** 448
[36] Ciappina M F, Cravero W R and Garibotti C R 2003 *J. Phys. B: At. Mol. Opt. Phys.* **36** 3775
[37] Pople J, Santry D and Segal G 1965 *J. Chem. Phys.* **43** S129
[38] Pople J and Segal G 1965 *J. Chem. Phys.* **43** S136
[39] Pople J and Segal G 1966 *J. Chem. Phys.* **44** 3289
[40] Siegbahn K *et al* 1969 *ESCA Applied to Free Molecules* (Amsterdam: North-Holland)
[41] Slater J C 1930 *Phys. Rev.* **36** 57
[42] Messiah A 1962 *Quantum Mechanics* vol 2 (Amsterdam: North-Holland)
[43] Tachino C A, Monti J M, Fojón O A, Champion C and Rivarola R D 2013 *Phys. Scr.* T **156** 014040
[44] Monti J M, Tachino C A, Hanssen J, Fojón O A, Galassi M E, Champion C and Rivarola R D 2013 *Appl. Radiat. Isot.* **83** 105
[45] Clementi C and Roetti C 1974 *At. Data Nucl. Data Tables* **14** 177
[46] Monti J M, Fojón O A, Hanssen J and Rivarola R D 2010 *J. Phys. B: At. Mol. Opt. Phys.* **43** 205203
[47] Monti J M, Fojón O A, Hanssen J and Rivarola R D 2010 *J. At. Mol. Opt. Phys.* **2010** 1
[48] Monti J M, Fojón O A, Hanssen J and Rivarola R D 2013 *J. Phys. B: At. Mol. Opt. Phys.* **46** 145201